Confinement effect in a quantum well dot induced by an InP stressor

J. Tulkki
Optoelectronics Laboratory, Helsinki University of Technology, Otakaari 1, FIN-02150 Espoo, Finland

A. Heinämäki
VTT Electronics, Otakaari 7B, FIN-02150 Espoo, Finland

(Received 25 May 1995)

We have calculated the confinement effect in an $In_{1-x}Ga_xAs/GaAs$ quantum well dot induced by a dislocation-free InP stressor island. The energy levels were calculated by including the strain interaction and the band-edge confinement in the Luttinger-Kohn Hamiltonian. The maximum level spacing for the dipole-allowed interband $E1 \rightarrow HH1$ line spectrum was 20 meV. Our calculation also gives excellent agreement with recent measurements [H. Lipsanen, M. Sopanen, and J. Ahopelto, Phys. Rev. B **51**, 13 868 (1995)] and provides indirect evidence of screened Coulomb interaction, tentatively addressed to slow carrier relaxation.

I. INTRODUCTION

Progress in experimental and theoretical study of quantum dots (QD), restricting the motion of electrons and holes in three dimensions, depends critically on the possibility to study the dynamics of separate discrete energy levels by various spectroscopic probes. To make such experiments feasible, there has been extensive research[1–4] to achieve a proper combination of the following "quality factors": (1) large confinement effect or level spacing, (2) homogeneous size distribution of QD's, and (3) elimination of surface and interface states and defects, which readily destroy a simple state structure.

Stressor-induced two- and three-dimensional confinement in the underlying quantum well (QW) should provide a special advantage regarding the property (3) since even when the stressor itself may contain defects, the potential well induced by the stressor is located in a region of a nearly perfect crystal. Small confinement effect (level spacing[1,3] $\approx 1-2$ meV) and the inhomogeneous broadening have, however, prevented the spectroscopy of separate levels, whenever several QD's are probed simultaneously. An approach to achieve a large confinement effect by self-organized Straski-Krastanow (SK) growth[5] was recently suggested by Sopanen and coworkers.[6] In their approach an InP island produced a level spacing ≈ 20 meV in a $In_{0.25}Ga_{0.75}As/GaAs$ quantum well dot.

In this work we report a complete computational analysis of the confinement effect in these quantum structures, shown schematically in Fig. 1. Our results, which include only material parameters of the pertinent bulk III-V materials are in excellent agreement with the $E1 \rightarrow HH1$ luminescence line spectrum reported by Sopanen *et al.*[6]

II. THEORY AND CALCULATIONS

The strain is calculated by determining a strain tensor $e_{i,j}; i,j = x,y,z$ for which the total strain energy $E = \int U(x,y,z)dV$ obtains the minimum value under appropriate boundary conditions. The strain energy density $U(x,y,z)$ in a zinc-blende structure can be expressed in terms of the elastic constants C_{11}, C_{12}, and C_{44}.[7] Elastic constants and all other material parameters used in the calculations are given in Table I. The strain was included in the finite element method (FEM) calculation by the ΔT method. The quantum structure was first assumed unstrained, all materials having the lattice constant of GaAs. Then the temperatures of the $In_{0.25}Ga_{0.75}As/GaAs$ QW and the InP island were

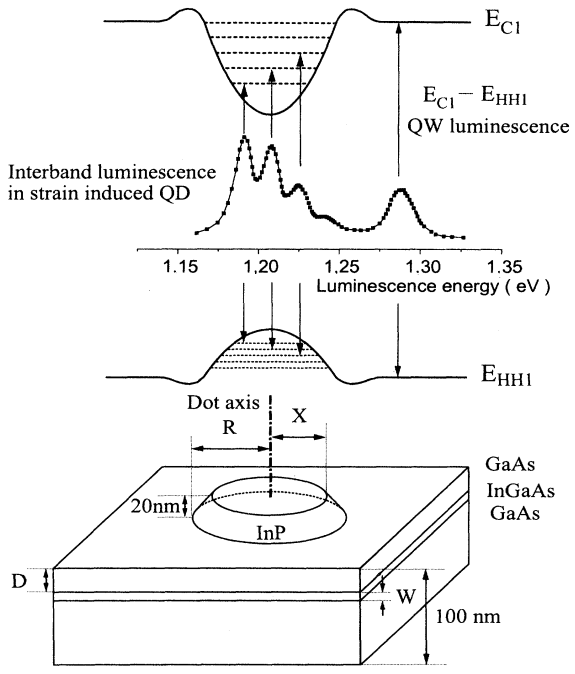

FIG. 1. The geometry of the strain-induced quantum dot and a schematic presentation of the luminescence spectrum including the $E1 \rightarrow HH1$ transitions in the QW and QD. In the middle we have shown a schematic experimental photoluminescence spectrum (Ref. 6).

 ©1995 The American Physical Society

TABLE I. Material parameters used in the calculations (Ref. 10). The band gaps and band offsets have been interpolated to $T=12$ K.

Parameter	Unit	GaAs	$In_{0.25}Ga_{0.75}As$
E_g	eV	1.520	1.163
V^e_{InGaAs} (from GaAs)	eV		0.276
V^h_{InGaAs} (from GaAs)	eV		0.081
γ_1		6.79	10.01
γ_2		1.92	3.54
γ_3		2.78	4.41
m_c	m_0	0.0665	0.0556
C_{11}	10^{11} dyn/cm^2	11.81	10.94
C_{12}	10^{11} dyn/cm^2	5.38	5.17
C_{44}	10^{11} dyn/cm^2	5.94	5.45
a_c	eV	−7.10	−6.68
a_v	eV	1.16	1.12
b_v	eV	−1.70	−1.73

artificially increased so that these materials obtained their real lattice constant. The total strain energy was then minimized by assuming that at the bottom of the 100-nm-thick structure as well as at sidewalls 200 nm away from the dot axis (see Fig. 1) the structure obtains the lattice constant of unstrained GaAs.

The strain interaction was calculated according to the theory of Pikus and Bir.[8,9] The strain interaction for the conduction band is given by the hydrostatic potential $V^e_H=a_c(e_{xx}+e_{yy}+e_{zz})$. Neglecting the spin-dependent terms, the strain Hamiltonian for the valence band is given by

$$H^h_{s-o}=\begin{bmatrix} V^h_H-V^h_S & S^* & -R & 0 \\ S & V^h_H+V^h_S & 0 & -R \\ -R^* & 0 & V^h_H+V^h_S & -S^* \\ 0 & -R^* & -S & V^h_H-V^h_S \end{bmatrix} \quad (1)$$

where the strain potentials are given by $V^h_H=a_v(e_{xx}+e_{yy}+e_{zz})$, $V^h_S=b_v[e_{zz}-(e_{xx}+e_{yy})/2]$, $R=(\sqrt{3}/2)b_v(e_{xx}-e_{yy})-id_ve_{xy}$, and $S=-d_v(e_{xz}-ie_{yz})$. The deformation potential constants a_c, a_v, and b_v are given in Table I. The nondiagonal terms R and S are not zero in our geometry except far away from the dot axis, where our structure approaches a strained QW, grown in the [001] direction. However, since the diagonal shear term V^h_S will decouple the heavy and light hole bands in the QD by approximately 100 meV, the correction of these nondiagonal terms in the strain Hamiltonian in Eq. (1) should be small near the band edge. Figure 2 displays the sum of the strain and band-edge confinement potentials seen by the electrons and heavy holes for a QD having $R=40$ nm, $W=8$ nm, $D=6$ nm, and $X=30$ nm. This particular combination of dimensions of the quantum well dot will be used as a reference and we will refer to it as QD0 in the following discussion.

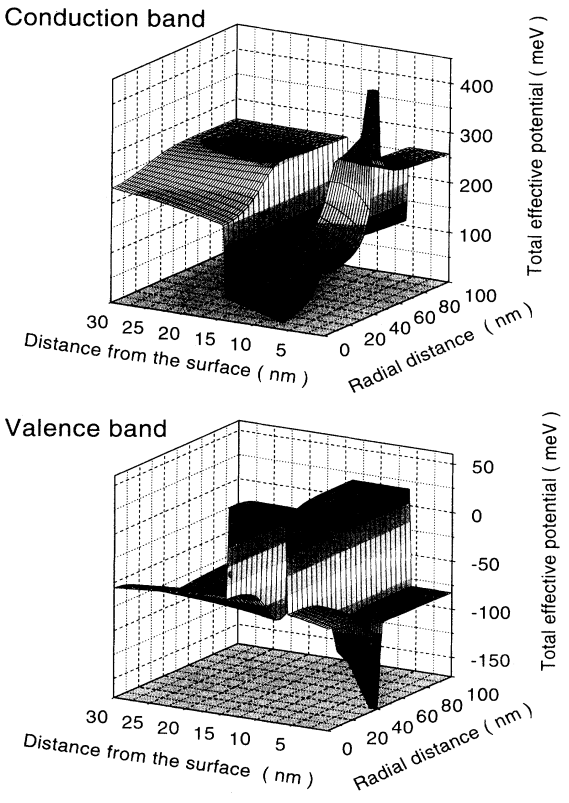

FIG. 2. The total confinement potential seen by the electrons (upper section) and heavy holes (lower section). The InP island is not shown. This figure corresponds to a QD structure having dimensions $R=40$ nm, $X=30$ nm, $D=6$ nm, and $W=8$ nm.

The calculation of the confinement effect was carried out separately for the QW and QD. We first calculated the conduction- and valence-band levels corresponding to the QW well away (≈ 150 nm) from the dot axis (see Fig. 1). In the calculation of QW energies we used the strain potentials corresponding to the distance of 150 nm from dot axis. At this distance the strain tensor is already very close to the asymptotic value of a lateral $In_{0.25}Ga_{0.75}As/GaAs$ QW grown on a very thick GaAs substrate. The off-diagonal strain potentials S and R in Eq. (1) are also very close to zero at $r=150$ nm.

The strain Hamiltonian Eq. (1) was added to the four-band Luttinger-Kohn Hamiltonian[9] and the conduction- and valence-band confinement energies, E^{QW}_{E1} and E^{QW}_{HH1}, respectively, were determined by solving the eigenvalue

problem by FEM. From the conduction- and valence-band confinement energies we obtain the $E1 \rightarrow HH1$ luminescence energy 1316 meV for a QW having the width $W=8$ nm and cladding layer $D=6$ nm. Our calculations neglect the indium segregation in the cladding layer. This would lower the barrier potential in the cladding layer and reduce the QW luminescence energy. Because of the compressive strain the shear interaction potential V_S^h will raise the heavy-hole band and lower the light-hole band, increasing their energy separation by about 100 meV in the QW. Since furthermore the first excited conduction-band state E_{E2}^{QW} is approximately 100 meV above the E_{E1}^{QW} level, we conclude that the near-band-gap absorption and emission are dominated by $E1 \rightarrow HH1$ transitions.

The confinement energies in the conduction and valence bands of the quantum well dot were calculated by using the cylinder coordinate system to make maximum use of the symmetry of the problem. Accordingly the total envelope function for electrons or holes was written as a factorized product $\Psi^{(e,h)}(r,z,\phi)=\psi_{n,m}^{(e,h)}(r,z)e^{i|m|\phi}$. Here $\psi_{n,m}^{(e,h)}(r,z)$ fulfills the eigenvalue equation

$$\left\{-\frac{\hbar^2}{2}\left[\left[\frac{\partial}{\partial z}\frac{1}{m_z^{(e,h)}(r,z)}\frac{\partial}{\partial z}\right]+\frac{1}{r}\left[\frac{\partial}{\partial r}\frac{r}{m_r^{(e,h)}(r,z)}\frac{\partial}{\partial r}\right]-\frac{1}{m_r^{(e,h)}}\frac{m^2}{r^2}\right]+V_{QW}^{(e,h)}(z)+V_{\mathrm{strain}}^{(e,h)}(z,r)\right\}\psi_{n,m}^{(e,h)}(r,z)=E_{n,m}^{(e,h)}\psi_{n,m}^{(e,h)}(r,z)\ . \tag{2}$$

In Eq. (2),

$$V_{\mathrm{QW}}^{(e,h)}(z)=V_{\mathrm{GaAs}}^{(e,h)}[Y(D-z)+Y(z-D-W)]+V_{\mathrm{InGaAs}}^{(e,h)}[Y(z-D)Y(D+W-z)]$$

is the band-edge confinement potential as a function of the distance from the surface. Here D and W are the dimension parameters and Y the step function. The strain potential $V_{\mathrm{strain}}^{(e,h)}(z,r)$ is equal to V_H^e or $V_H^h+V_S^h$ for electrons and holes, respectively. For electrons $m_r^e=m_z^e=m_c$, whereas for holes the lateral and vertical masses are given by $m_r^h=1/(\gamma_1+\gamma_2)$ and $m_z^h=1/(\gamma_1-2\gamma_2)$, respectively. In Eq. (2) we have neglected the coupling of HH and LH bands included in the Luttinger-Kohn Hamiltonian to make the problem numerically two dimensional. However, as pointed out above the HH and LH bands are separated by the V_S^h strain potential, which decreases the effect of band coupling. In the following we have labeled the different angular momentum states by Σ,Π,Δ,Φ for $|m|=0,1,2,3$, etc., respectively. In analogy to the theory of a two-dimensional harmonic oscillator there is always one Π state between two Σ levels. If the potential would be exactly harmonic, we would have $E_{n\Sigma}^{(e,h)}=E_{(n-1)\Delta}^{(e,h)}$ and $E_{n\Pi}^{(e,h)}=E_{(n-1)\Phi}^{(e,h)}$, etc. We found that for low n and m these equations are rather accurately fulfilled, whereas for higher rotational levels we found a splitting of 1–2 meV. This splitting is caused by the large centrifugal barrier, which drives the electrons and holes from the dot axis to the outer region, where the harmonic approximation is not valid.

III. RESULTS AND DISCUSSION

The zeroes of the potential-energy scales in Fig. 2 were set to the band edges of the unstrained $In_{0.25}Ga_{0.75}As$. For both electrons and holes, there is an extremum, minimum for electrons and maximum for holes, in the QW below the InP stressor, indicating that electrons and holes are diffused to these local extrema and relaxed to bound QD states before finally recombining radiatively. In the vicinity of the dot axis the effective potential as a function of r (for fixed z) is approximately harmonic. In Fig. 2 the conduction-band minimum is 96 meV below the bottom of the QW band edge and the valence-band maximum is 19.7 meV above the top of the QW band edge. We found a large variation in the ratio of

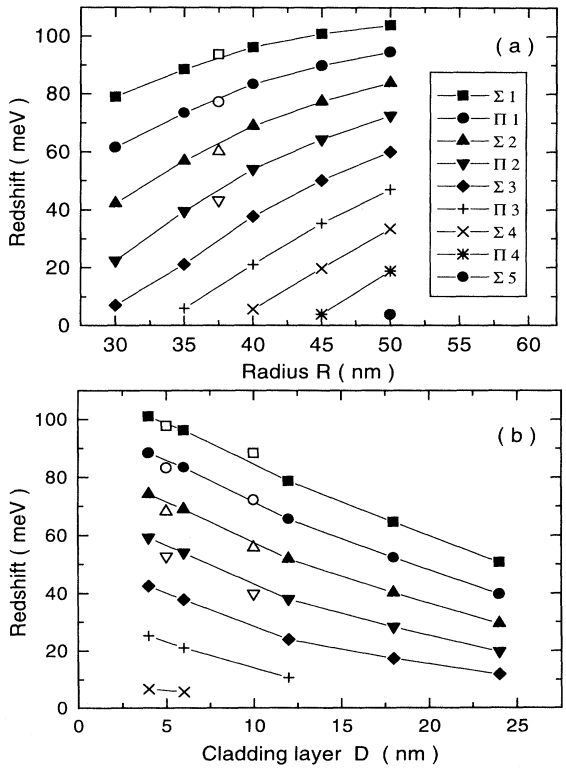

FIG. 3. (a) The redshifts (from the $E1 \rightarrow HH1$ QW luminescence line) of the interband Σ and Π transitions as a function of the dot radius R. In this calculation $X=R-10$ nm, $W=8$ nm, and $D=6$ nm. (b) The redshifts as a function of the thickness of the cladding layer D for fixed $W=8$ nm, $R=40$ nm, and $X=30$ nm. Open symbols are experimental data from Ref. 6.

confinement energies $E^h_{n,m}/E^e_{n,m}$. The maximum value of 0.71 was obtained for a thick cladding layer ($R=40$ nm, $D=18$ nm) and the minimum 0.22 for a large InP island and thin cladding layer ($R=50$ nm, $D=4$ nm). This large variation in the sharing of the confinement effect between electrons and holes should be useful in the experimental study of carrier relaxation in the QD's.

We define the redshift as the energy difference between the QD interband $E1\rightarrow HH1$ luminescence energy from the corresponding QW transition energy. This difference is given by $E_{Rn,m}=E^{\mathrm{QW}}_{E1}-E^e_{n,m}-E^{\mathrm{QW}}_{HH1}+E^h_{n,m}$, where all energies are measured from the band edges in the QW. We use the label $E1\rightarrow HH1$ even for the set of dipole-allowed QD luminescence lines, since the electron and hole wave functions (not shown) clearly exhibit the single vertical mode that is characteristic of the corresponding QW states. Figure 3 shows the redshifts of interband $E1\rightarrow HH1$ transitions as a function of R and D. We use QD0 as a reference and change one of the parameters, R or D, at a time, while keeping the other dimensions fixed to their values in QD0.

The calculated redshifts are in excellent agreement with measurements of Sopanen and co-workers.[6] In Figs. 3(a) and 3(b) we have shown the experimental data by open symbols. We have used $R=37.5$ nm for experimental data in order to account for a more accurate determination of the InP island radius.[6] The experimental values were interpolated to correspond to $W=8$ nm by auxiliary calculation of the redshift as a function of W. When we used $D=6$ nm and $W=8$ nm the largest calculated level spacing was ≈ 20 meV and the largest redshift 102 meV.

The dipole-allowed interband $E1\rightarrow HH1$ transition amplitudes are proportional to overlap integrals $\langle \Psi^e_{n,m}(r,z,\phi)|\Psi^h_{n',m'}(r,z,\phi)\rangle$. In Fig. 4 we present the overlap integrals between Σ (odd indices) and Π (even indices) states for the reference dot QD0. The transitions with $m\neq m'$ are also marked in Fig. 4 although these integrals are exactly equal to zero. The electron and hole states are orthogonal to a very high accuracy (for the lowest states $\langle \Psi^e_{n,m}|\Psi^h_{n,m}\rangle \approx 0.998$). Only for the higher states is there some nonorthonormality. The 4Σ state (number 7 in Fig. 4) is an exception, since this electron level is above the E^{QW}_{E1} energy and can decay by tunneling to the QW.

Our calculation corresponds to a complete screening of Coulomb interaction. For strong confinement, recent calculations by Bockelmann and co-workers,[11] including Coulomb interaction, predict a large deviation from the even spacing of levels typical to the harmonic potential approximation. By contrast, the experimental level spacing has been found to remain constant and regular also at high excitation intensity.[6] The state filling resulting from the increasing excitation intensity[6] should have had a large effect on exciton states predicted by Bockelmann.[11] The screening of Coulomb interaction could be explained by a fast diffusion of electrons and holes to QD's followed by slow relaxation to bound levels. Since the dots cover only a small fraction of the surface the density of the screening charge at QD's can become rather high even at low excitation intensity. Thus the good agreement between our calculations and the experiment,[6] and the absence of intensity dependence of energy levels in the experiment, support indirectly the existence of the *phonon bottleneck*[12] effect, i.e., the slow relaxation of electrons and holes to bound levels before radiative recombination.

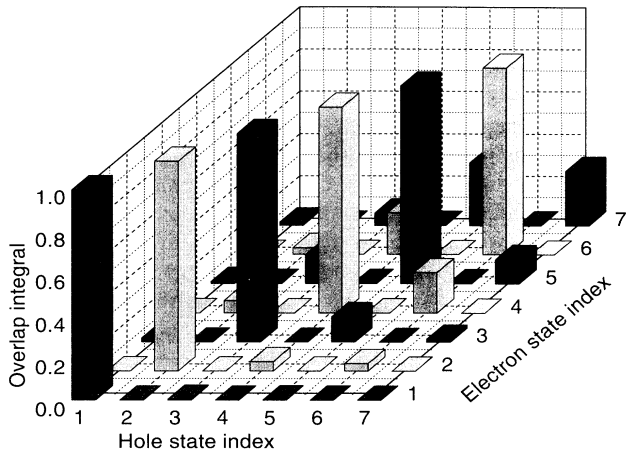

FIG. 4. The absolute values of the overlap integrals $\langle \Psi^e_{n,m}|\Psi^h_{n',m'}\rangle$ between the electron and heavy-hole envelope wave functions. The selection rules for interband transitions are governed by the squares of the overlap integrals. In this figure the odd state indices correspond to Σ states and even indices to Π states.

In conclusion, we have shown that a model based on strain-induced confinement and the Luttinger-Kohn theory can explain the most salient features in the luminescence spectrum of quantum well dots fabricated by SK growth method. A more complete calculation accounting for Coulomb interaction, the *HH-LH* coupling and including a study of relaxation mechanisms is in progress.

ACKNOWLEDGMENTS

This work has been largely inspired by the experimental work of M. Sopanen, H. Lipsanen, and J. Ahopelto. We gratefully acknowledge having results of their experimental work at our disposal prior to publication and their numerous comments on this work. We also thank Timo Kahala and Sami Saarinen for assistance in the strain calculations. This work was funded by the Academy of Finland.

[1] K. Kash, B. P. Van der Gaag, D. D. Mahoney, A. S. Gozdz, L. T. Florez, J. P. Harbison, and M. D. Sturge, Phys. Rev. Lett. **67**, 1326 (1991).

[2] K. Kash, D. D. Mahoney, B. P. Van der Gaag, A. S. Gozdz, J. P. Harbison, and L. T. Florez, J. Vac. Sci. Technol. B **10**, 2030 (1993).

[3] I-Hsing Tan, M. Y. He, J. C. Yi, E. Hu, N. Dagli, and A. Evans, Appl. Phys. Lett. **62**, 1376 (1993).

[4]J.-Y. Marzin, J.-M. Gerard, A. Izrael, D. Barrier, and G. Bastard, Phys. Rev. Lett. **73**, 716 (1994).

[5]D. J. Eaglesham and M. Cerullo, Phys. Rev. Lett. **64**, 1943 (1990).

[6]M. Sopanen, H. Lipsanen, and J. Ahopelto, Appl. Phys. Lett. **65**, 1662 (1995); H. Lipsanen, M. Sopanen, and J. Ahopelto, Phys. Rev. B **51**, 13 868 (1995).

[7]C. Kittel, *Introduction to Solid State Physics,* 4th ed. (John Wiley, New York, 1971), p. 140.

[8]G. E. Pikus and G. L. Bir, Fiz. Tverd. Tela **1**, 1642 (1959) [Sov. Phys. Solid State **1**, 136 (1959)].

[9]T. B. Bahder, Phys. Rev. B **41**, 11 992 (1990).

[10]*Semiconductors. Physics of Group IV Elements and III-V Compounds,* edited by K.-H. Hellwege and O. Madelung, Landolt-Börnstein, New Series, Group III, Vol. 17, Pt. a (Springer, New York, 1982); *Semiconductors. Physics of II-VI and I-VII Compounds, Semimagnetic Semiconductors,* edited by K.-H. Hellwege and O. Madelung, Landolt-Börnstein, New Series, Group III, Vol. 17, Pt. b (Springer, New York, 1982).

[11]U. Bockelmann, Phys. Rev. B **48**, 17 637 (1993); U. Bockelmann, K. Brunner, and G. Abstreiter, Solid State Electron **37**, 1109 (1994).

[12]H. Bensity, C. M. Sotomayor-Torres, and C. Weisbuch, Phys. Rev. B **44**, 10 945 (1991).

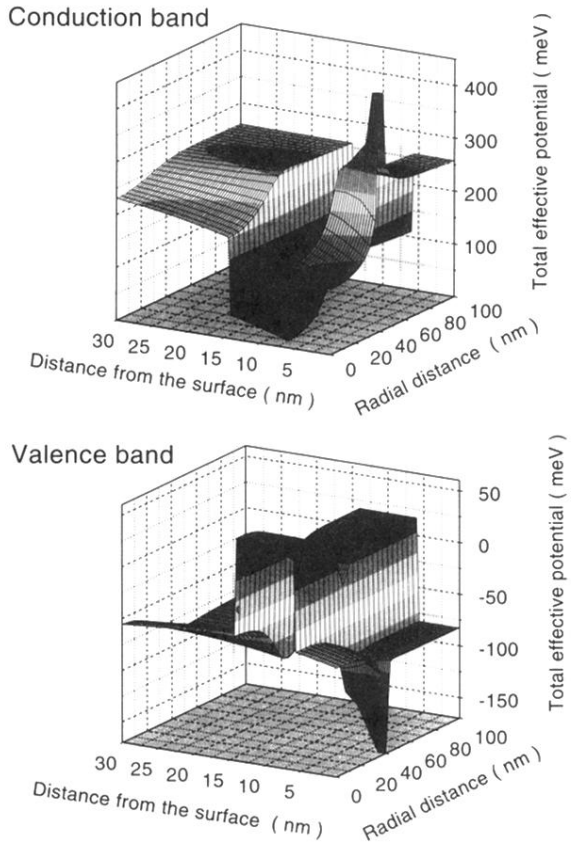

FIG. 2. The total confinement potential seen by the electrons (upper section) and heavy holes (lower section). The InP island is not shown. This figure corresponds to a QD structure having dimensions $R = 40$ nm, $X = 30$ nm, $D = 6$ nm, and $W = 8$ nm.

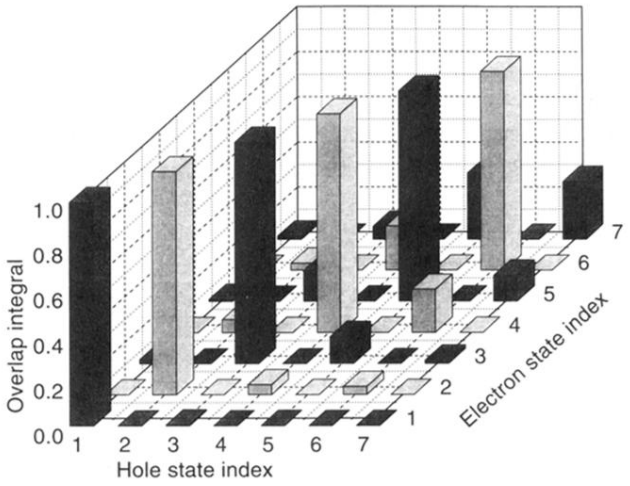

FIG. 4. The absolute values of the overlap integrals $\langle \Psi^e_{n,m} | \Psi^h_{n',m'} \rangle$ between the electron and heavy-hole envelope wave functions. The selection rules for interband transitions are governed by the squares of the overlap integrals. In this figure the odd state indices correspond to Σ states and even indices to Π states.